

*By Charles Malo, University of Ottawa Heart Institute, Ottawa, Ontario, Canada
With supervision by Robert A. deKemp and Ran Klein*

May-August 2009

Keywords: FlowQuant, UNIX, Left Ventricle, Ejection Fraction, Volume, Wall Thickening, Myocardium, PET

Table of Contents:

A. Abstract

B. Left Ventricle Ejection Fraction & Wall Thickening Calculation

I. Introduction

II. Methodology

1) Acquiring the data: Background on PET Imaging

2) Processing the data

3) Improving the report page

4) Facts

III. The Calculations

1) Basic calculation of LV volumes ignoring Wall Thickening

2) Calculating Wall Thickening by Iteration

3) Recalculation of volumes and Ejection Fraction considering Wall Thickening effect

IV. FlowQuant to 4DM Comparison and Discussion

C. UNIX Support Feature

I. Introduction

II. Methodology

1) Case Sensitivity Mismatch

2) Backward/Forward slash dilemma

3) UNIX paths and tools

III. Limitations

D. Conclusion

E. Copyrights and Acknowledgements

F. References

G. Confidentiality Release

A. Abstract

For my first work term (SEG 2901), completed from May to August 2009, I was employed as a software developer of new methods and visualization tools for the FlowQuant software program which studies the heart's *Left Ventricle* functionality using positron emission tomography (PET) images. My duties were to create, assisted by both supervisors, various algorithms which can facilitate the diagnosis of the heart disease, thus determining proper treatments. In particular, I was asked improve the accuracy of an algorithm for measuring the *Ejection Fraction*, an estimation of the heart efficiency, from electro cardiogram (ECG) gated PET images. The accuracy improvement was addressed by estimating the myocardium *wall thickening* and validated using a clinically accepted program (4DM). FlowQuant is written to be as *universal* and *automated*, as possible, with minimal *assumptions*. A secondary task was to modify the software to *run on UNIX and Windows platforms*.

B. Left Ventricle Ejection Fraction & Wall Thickening Calculation

I. Introduction

Positron Emission Tomography (PET) has become an “important non-invasive technique in cardiovascular research, offering unique insight into biochemical changes on a molecular level with excellent sensitivity” ⁽¹⁾. The Ejection Fraction (EF), an estimation of the heart's efficiency, is an important factor in diagnosis and determining proper treatment. It has been shown that PET perfusion images can be used to estimate the Wall Thickening (WT) throughout the Left Ventricle (LV) myocardium beating cycle, thus adding more accuracy to the Ejection Fraction calculations. The FlowQuant (FQ) software program, developed at the University Of Ottawa Heart Institute (UOHI), has the functionality to accept Digital Imaging and Communications in Medicine (DICOM) images and various other types of scans as an input, process them in different ways, and show graphical outputs providing information on the heart's functionality. During the summer of 2009, this program has been updated with functionality to measure Ejection Fraction and Wall Thickening, thus improving its clinical and research utility.

II. Methodology

1) Acquiring the data: Background on PET Imaging:

“Positron emission tomography (PET) is a nuclear medicine imaging technique which produces a three-dimensional image or picture of functional processes in the body. The system detects pairs of gamma rays emitted indirectly by a positron-emitting radionuclide (tracer), which is introduced into the body on

a biologically active molecule. Images of tracer concentration in 3-dimensional space within the body are then reconstructed by computer analysis.^{»(2)}

These PET images are acquired by injecting the patient with a small amount of radioactive substance (called a tracer) such as ^{18}F FDG glucose or Rubidium (^{82}Rb) and imaging using a specialized PET camera which reconstructs images of the tracer distribution. That tracer is carried by the blood flow into the patient's heart, where it is absorbed by the myocardium wall (the heart muscle).

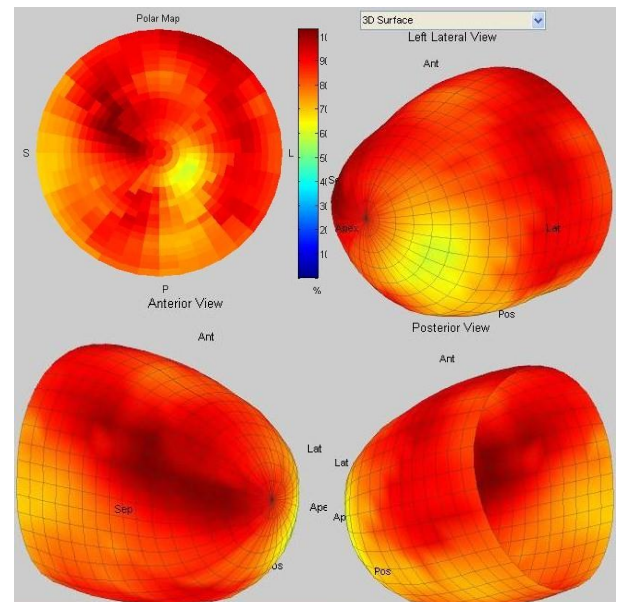
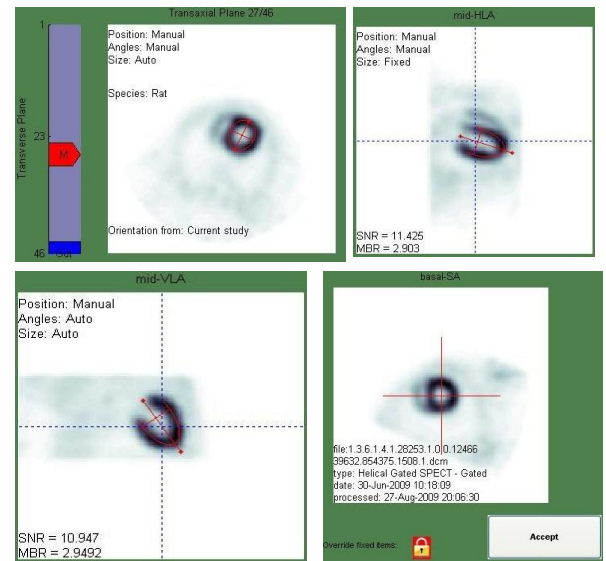
The images taken of the radioactive uptake using the PET camera are then stored into DICOM files, where all values and entries of the patient's information are saved as well, for later use by a proper software program such as FlowQuant or 4DM (Invia, Ann Arbor, Michigan, USA). Once all the clinical data as well as the uptake images in the heart muscle are stored, the scans are loaded into FlowQuant, which analyses them based on what the user wishes to study.

2) Processing the data:

One of the important features available in FlowQuant is a mid-myocardium contour detection based on the highest uptake points in the muscle, allowing a rough estimation of the mid-myocardium coordinates in x, y, and z directions. Based on the coordinates of the points delimiting the mid-myocardium, radii values are estimated, and written in a structure variable, containing all properties of the LV, for later use. Since the heart changes shape during the cardiac cycle, for each of the 8 frames (representing 8 different cardiac interval snapshots), different radii values and phase-dependant variables are detected for each one of these phases.

Prior to the Gated Report, along each axis, the images are averaged out throughout all the gates, and an automated mid myocardium wall detection occurs to delimit the LV shape for the rest of the study. The user can also override the automated detection for quality assurance. Then the sample wall detection is applied on all gates automatically. This process is entitled "LV Sampling"; Polar Maps and 3D Surface plots can be created as from now.

While FlowQuant was designed to analyze static and dynamic images, it only had basic functionality for analyzing gated images. The "Gated Report" which was implemented as a starting point, which had the functionality of acquiring variables created or stored during the execution of the analysis. From those variables, including the radii stored, that function could create a very rough and rigid animated surface



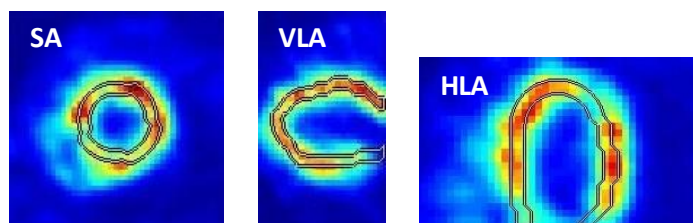
plot, as well as display slices of the LV at different view angles along the Short Axis (SA), Horizontal Long Axis (HLA) and Vertical Long Axis (VLA).

3) Improving the report page:

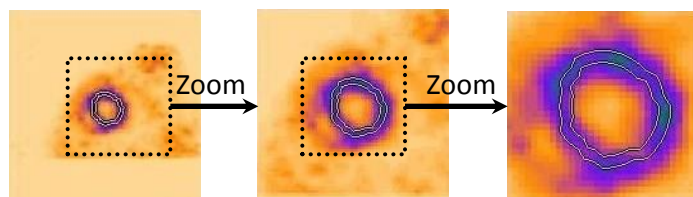
The first priority was to design a new report page that is user-friendly, attractive to the eye, contains appropriate functionality, and provides the vital information the researchers and clinicians require. The report window is interactive and loops through the image gates. A separate report window is displayed for each image and all the windows are synchronized to enable comparison between scans. The new figure for each study is now divided into somewhat four quadrants distinguished by the type of their contents: LV Slices, LV Gated Model, LV Polar Maps (PM), and Graphic Curves.

❖ LV Slices:

The LV slices are animated views of the LV wall at three different angles, showing the wall movements throughout the cardiac cycle, based on the radioactive uptake in the muscle itself.



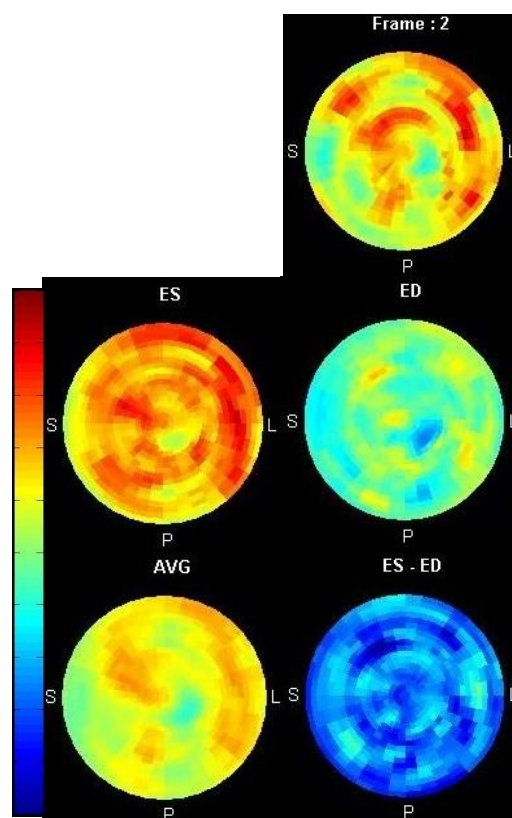
All of the SA, HLA, and VLA slice images are stretched to fit their respective axes keeping aspect ratio. Inner and outer myocardium wall contours are added to the slices, with an option to turn their display off. These contours are implemented to follow the wall motion, and to accommodate the use of the zoom slider option by updating the contours to fit to wall borders.



❖ LV Polar Maps:

An LV polar map is considered as a flattened version of the model, a disk view of the LV along the SA, centered at the Apex.

Four static polar maps are created using the uptake values stored: the ED Polar Map (ED PM), ES Polar Map (ES PM), Average Polar Map (AVG PM) and the Wall Thickening Polar Map (WT PM). The WT PM is represented by the subtraction of the ED PM from the ES PM, the reason is that the muscle shows more intensity in ES when it is thick and contracted,



rather than in ED where the muscle is thinner and dilated. Thus the difference in intensity between both polar maps is related to, not measured by, the change in wall thickness. A fifth PM is also added to the figure which is animated phase by phase.

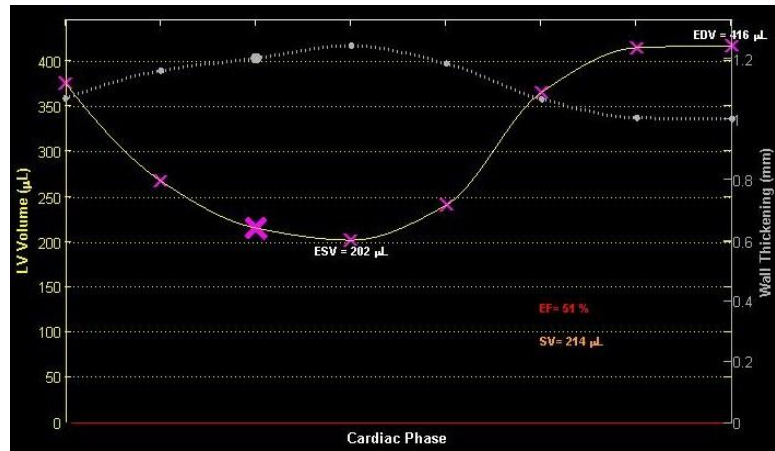
❖ Graphic Curves:

After the volume of the LV at each frame is calculated using the algorithm described later on, these values are plotted in the graph and an estimated curve is drawn linking these points by interpolation.

Another curve is plotted similarly for the estimated Wall Thickening.

A highlighted mark on each curve is animated to follow the curve's trajectory based on the current frame.

The graph also views the calculated End Diastole Volume (EDV), End Systole Volume (ESV), Ejection Fraction (EF) percentage and Stroke Volume (SV).

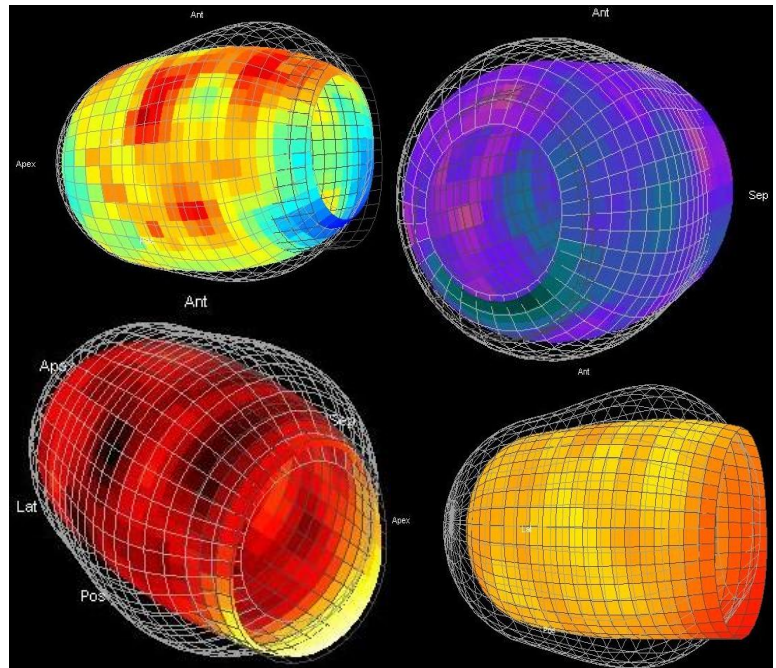


❖ LV Gated Model:

The LV model is updated with new features among like the 3D rotation ability.

Smoothing of the surface plot was associated with the plotting function, interpolating the radii values along smaller steps to draw a smoother and more even model of the LV, giving it a nice and soft vase shape.

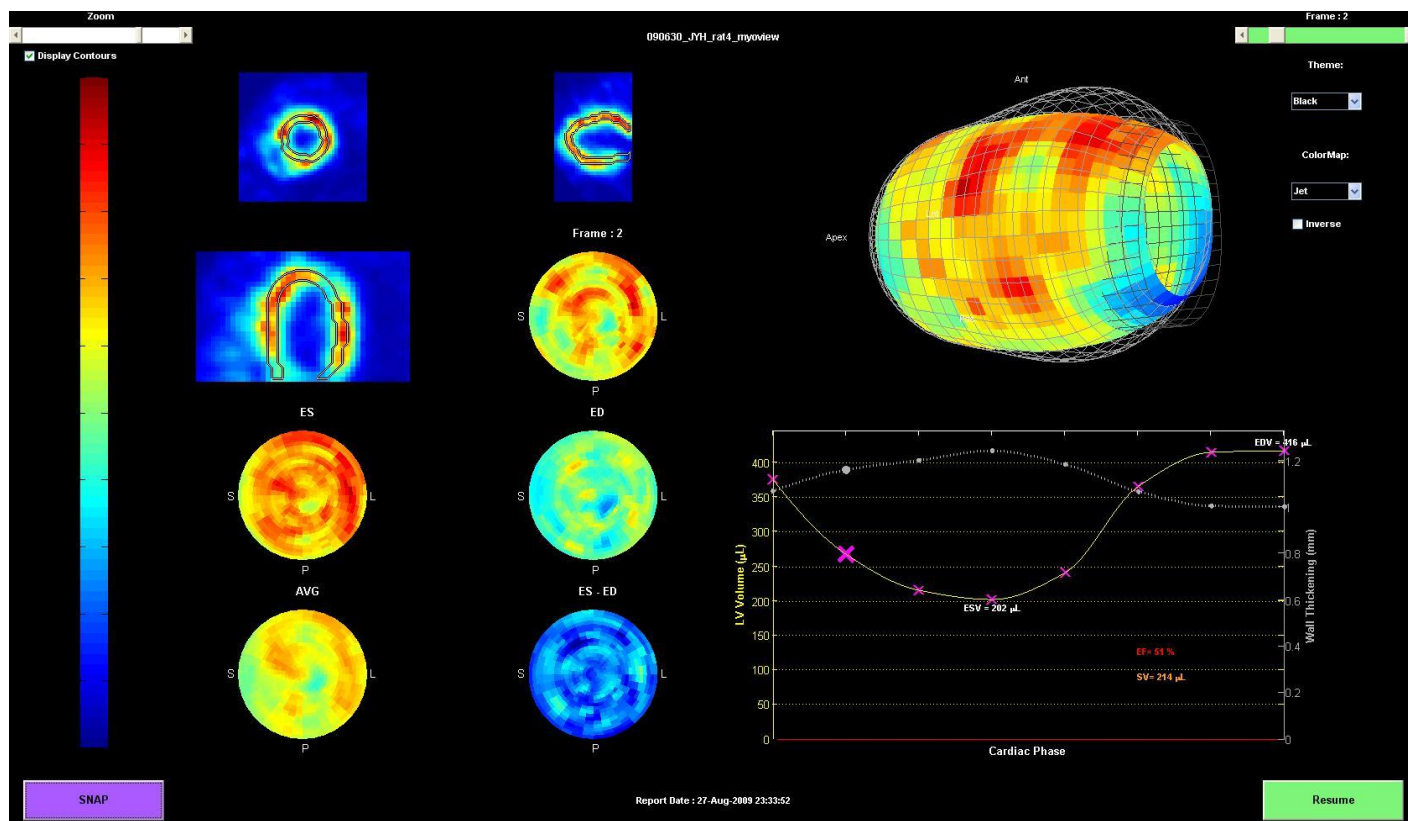
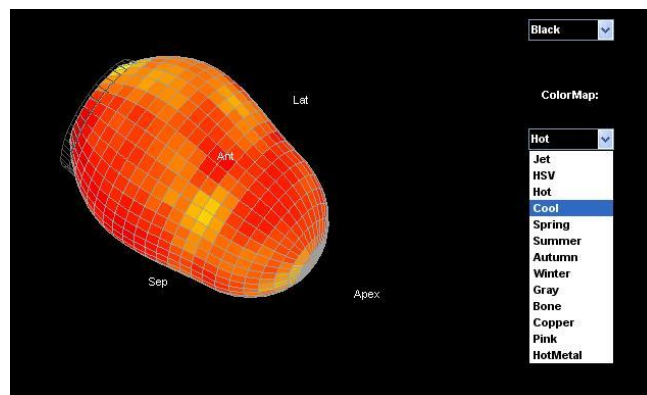
After determining the End Diastole (ED) and End Systole (ES) frames and obtaining the specific radii at those frames by a process explained later on in the report, their respective meshes were added to the surface plot, on the same axis. These meshes represent respectively the maximum and the minimum size and shape the left ventricle can take during the cardiac cycle. Having those fixed delimiting plots, the user can now have more insight on the LV wall motion and shape in respect to those grids.



❖ GUI controls:

Various GUI control were added to the figure to manage the output on the figure, among which are:

- ✚ A slider to control the zoom of the slice images, and a display toggle button to show the myocardium wall contours or not.
- ✚ A Frame Rate slider to control the animation speed of the entire figure.
- ✚ A theme List to alter the style of the figure between, so far, the default grey theme and the more appealing black theme.
- ✚ A Color Bar is associated with the currently selected Color Map to view the range of the colors used.
- ✚ A capture button was added in order to save a video capture of the entire animated figure throughout a complete cardiac cycle, offering different formats for the video output ('avi', 'mpeg', or 'gif'). When the animation is paused, the video capture button works as a snapshot button that can save an image file (in 'jpg' format) of the figure at the current phase.
- ✚ A Pause button can temporary stop the animations in the figure, also it transforms the Frame Rate slider to a frame selector, which enables the user to chose which phase of the cycle he wishes to view.
- ✚ A Color Map List to modify the colors and their ranges used to display the graphical outputs and the ability to inverse the colors.



4) Facts:

- Fact 1: The volume of the LV is larger at end diastole, and smaller at end systole.
- Fact 2: The myocardium wall is the thinnest at end diastole where it is dilated, and the thickest at end systole, where the muscle is contracted.
- Fact 3: As consequence to fact 2, the intensity in the myocardium is the highest at end systole and lowest at end diastole due to partial volume loss.
- Fact 4: The highest intensity in the muscle is recorded along the mid-myocardium wall.
- Fact 5: If the mass of an object and its density do not change its volume is constant regardless of its shape.
- Fact 6: The myocardium wall thickness is not uniform at all points in the wall, and the thickness changes during the cardiac cycle.
- Fact 7: The mid myocardium line is not necessarily
- Fact 8: A volume of an object is the integrated sum of the area of thin slices of that object along its axis.

III. The Calculations

I. Basic calculation of LV volumes ignoring Wall

Thickening:

During the cardiac cycle, the LV changes shape and size when contracting and expanding, thus the mid myocardium reference points vary at each frame. Therefore, radii values stored for each frame aren't constant throughout the cycle, they grow until ED, and shrink till ES.

FlowQuant analyses the LV, and treats it as a 3D model that can be divided along the short axis into slices, called "Rings" in the Gated Report, even if they are not symmetric or geometric.

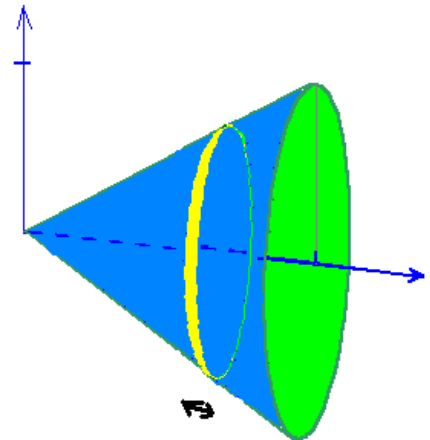
To calculate the LV blood volumes, having a best fit function of the 3D model causes major accuracy loss due to partial volume loss and low edge detection efficiency in PET imaging.

Therefore, the alternate idea was to calculate the model's volume through an integration of the area of one-pixel-spaced slices along the SA. The slices would be treated as planar polygons.

The LV cavity area at each slice, defined by the polygon's area, is calculated, and integrated along the SA to determine the volume of the cavity, thus the blood capacity. Note that at this point, the volume calculated is not pure cavity volume only, but also contains a partial volume of the myocardium wall because of Wall Thickening disregard.

Fortunately, a pre-defined Matlab function ("poly2mask") can convert a region-of-interest polygon into a binary region of interest (ROI) mask. A mask is similar to a binary matrix of m by n dimensions that represents the ROI polygon. "The function sets pixels in the mask that are inside the polygon to 1 and sets pixels outside the polygon to 0.

When creating a region of interest (ROI) mask, poly2mask must determine which pixels are included in the region. This determination can be difficult when pixels on the edge of a region are only partially covered by the border line" ⁽³⁾, yet an internal "self-correcting" algorithm will



verify whether the partial pixel is within the ROI or not, thus it is relatively safe to assume that it neither overestimate nor underestimate the ROI computed.

Once the binary mask is created, entries containing ones represent the area of the polygon at each slice. Then a sum of all the entries containing Ones of all slices' masks (integrating along SA slice by slice, using fact 7) will represent approximately the number of pixels that fill the shape. Multiplying the number of pixels estimated with the volume of one unique pixel will result in finding the volume of the cavity, in units of pixels, which is then converted into milliliters or micro liters depending on the subject's species type. This is how any volume calculations are done in this program, using in this case radii unaffected by Wall Thickening at each phase. The stroke volume can be calculated at this point; it is defined as the positive difference between the ED and ES volumes:

$$SV = EDV - ESV.$$

Also the Ejection Fraction is defined by the ratio of the Stroke Volume to the End Diastole Volume:

$$EF (\%) = (SV/EDV)*100 \quad \text{or} \quad EF (\%) = (EDV - ESV/EDV)*100$$

However, the values computed show an under estimation of a large degree in comparison with the results derived in 4DM.

Essentially, the need of the currently rough volume calculations is to guess what frames represent the ED and ES frames to carry on with the next step.

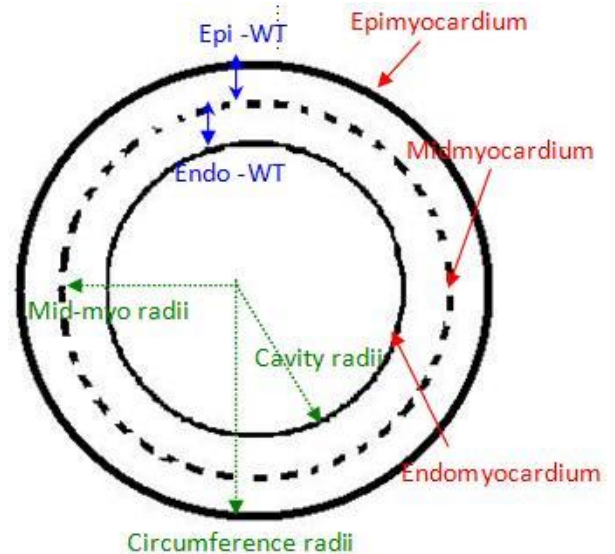
II. Calculating Wall Thickening by Iteration:

Finding the ED frame is an easy conjecture, it is determined by the frame that represents the highest estimated volume, from Fact 1.

The radii values stored are measured up to the mid myocardium. A small assumption is made: the inner (Endo) wall and the outer (Epi) wall border are equidistant to the mid myocardium line, thus the Endocardium and Epicardium wall thicknesses are both equal to half the total wall thickness at each frame.

$$(Epi\ WT = Endo\ WT = total\ WT/2)$$

Note: Figure on the right is a representative drawing of a SAs slice not a real image.



Since no pre-existing Wall Thickening measurement algorithm was available on hand, I had to develop my own one. An iterative approach is sought. Using all the data stored at the ED frame, I aimed to calculate the volume of the myocardium wall using the same volume calculating algorithm, and both of these sets of radii: the inner wall radii and outer wall radii.

Subtracting the Endo WT from the mid myocardium radii at each frame results in finding the radii defining the inner wall contour, thus the borders of the LV cavity. In addition, adding the Epi WT to the mid myocardium radii, at each frame, results in getting the radii defining the outer wall contour, thus the circumference of the LV. Applying the volume calculating algorithm leads in finding respectively the cavity volume as well as a total volume of the LV at the ED frame.

The myocardium wall volume is then computed by subtracting the first smaller volume from the second larger volume.

The wall volume calculated is assumed to be the real and constant volume of the myocardium wall throughout all the phases (Fact 5) even though another small assumption is made regarding the Wall Thickness at that level.

It is assumed, for now, that the Wall Thickness is uniform all over the myocardium wall, and its value at end diastole is a specific clinical averaged value depending on the species type of the subject studied. For example, at End Diastole, a human LV wall is assumed to be 10mm thick, a rat's WT of 1mm, a mouse's WT of 0.5mm and so on.

Understanding Fact 2, this WT value is considered as the minimum WT value, and thus a starting point to calculating the other WT values for the other phases of the cycle.

Having at this point the assumed real, precise and constant volume of the myocardium wall, the mid myocardium radii for all phases and the minimum starting point for the wall thickening, an algorithm is created that does the following process for each frame:

For each set of radii at each frame, starting with the minimum value of the WT (i.e. the ED WT using fact 1) and iteratively increasing it with a growing step size on each iterative call, the function calculates a trial wall volume by means of the process described above, using the updated radii (i.e. radii from which the WT was subtracted). The calculated wall volume will grow in a loop until it becomes equal to the assumed real constant wall volume pre-calculated at the ED. At this point, the function will return the current wall thickening value used with that set of radii that gave the best match, and stores it in a variable for later use. This is the iterative approach of calculating the wall thickening. Another theory sought is to divide the constant wall volume by the surface area of the model at each frame, and thus acquiring the wall thickness instantly, yet the surface area calculation is harder due to the limitations of the resolution of the PET perfusion scans such as partial volume loss.

Either way, the wall thickening is still assumed uniform at all reference points of the myocardium wall.

III. Recalculation of volumes and Ejection Fraction considering Wall Thickening effect:

Subtracting the recently calculated Wall Thickening values at each frame from its respective radii set, the volume calculation algorithm is invoked once more, and the new volume results are assumed to be the true volumes of the LV cavity, therefore the amount of blood contained in that cavity at each cardiac phase. A more accurate Ejection Fraction can now be calculated, and the results computed can now be compared with the currently acknowledged program 4DM.

Additional detail on Calculation Methods:

FlowQuant assumes a fixed valve plane when computing the volumes, yet it is intended later on to acquire the feature to detect the valve plane location and incline for each frame. FlowQuant used to crop the edge of the LV at the 18th Ring from the apex to accommodate the actuality of a moving plane. Yet to compare with 4DM, being mostly manual and taking into account the moving plane, FlowQuant was temporarily manipulated to run a trial computation of all results for each number of rings from 18 to 24, in order to get more insight on the volume calculation process in 4DM and how the number of rings considered slightly affects the comparison results as shown later.

IV. FlowQuant to 4DM Comparison and Discussion:

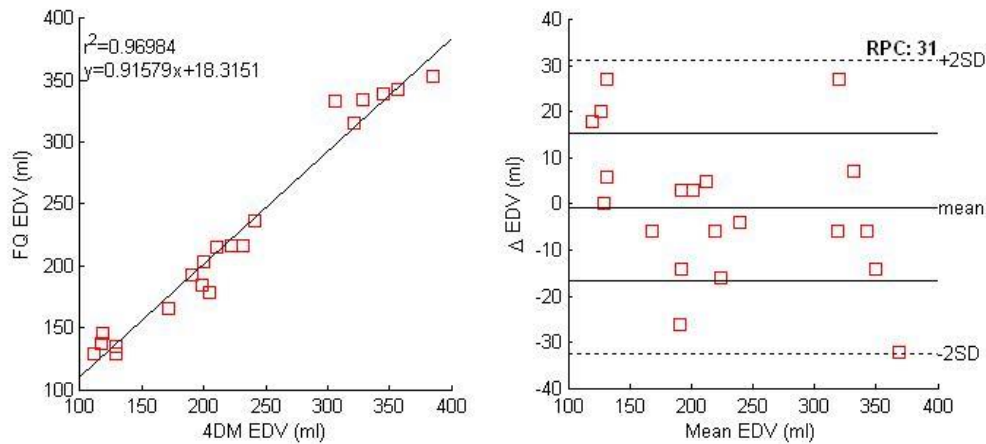
Lack of time being an issue, only twenty human scans were randomly selected from the Hospital's scans archives to run the comparison test between the FlowQuant and 4DM LV analysis programs. Each scan was processed in 4DM as well as in FlowQuant by me, and the results computed were stored in a comparison table and studied for their correlation using the Bland-Altman analysis method. Note that the age of most patients was, by pure hazard, high: the age range goes from 46 to 87 years old, with a mean value of about 66 years. Also, usually most patients who are referenced to an FDG scan, such as the ones analyzed in this report, are presumed to have a certain heart disease or flawed functionality, therefore these determined EF values are relatively lower than average. Patients' names are concealed to preserve the hospital's confidentiality.

<u>CASE</u>					<u>FLOWQUANT</u>				<u>4DM</u>			
<u>Patient</u>	<u>Species</u>	<u>SEX</u>	<u>AGE</u>	<u>Volume UNITS</u>	<u>EDV</u>	<u>ESV</u>	<u>SV</u>	<u>EF (%)</u>	<u>EDV</u>	<u>ESV</u>	<u>SV</u>	<u>EF (%)</u>
*****	Human	Male	73	mL	129	66.2	62.5	49	111	67	44	40
*****	Human	Male	68	mL	203	160	43	21	200	159	41	21
*****	Human	Female	46	mL	215	153	62.2	29	210	157	53	25
*****	Human	Male	52	mL	178	143	35.6	20	204	161	43	21
*****	Human	Female	82	mL	135	94.2	40.5	30	129	88	41	32
*****	Human	Male	87	mL	216	164	51.8	24	222	153	69	31
*****	Human	Male	54	mL	343	302	41.4	12	357	306	51	14
*****	Human	Male	55	mL	353	316	37.1	11	385	341	44	11
*****	Human	Female	84	mL	335	314	21.2	6.3	328	312	16	5
*****	Human	Male	68	mL	193	141	52	27	190	137	53	28
*****	Human	Female	70	mL	145	93.9	50.9	35	118	63	55	47
*****	Human	Female	58	mL	137	125	12	8.8	117	100	17	15
*****	Human	Female	58	mL	165	121	43.9	27	171	127	44	26
*****	Human	Male	80	mL	216	167	48.1	22	232	156	76	33
*****	Human	Male	47	mL	129	105	23.7	18	129	102	27	21
*****	Human	Male	65	mL	316	263	53.4	17	322	271	51	16
*****	Human	Male	77	mL	185	159	25.7	14	199	171	28	14
*****	Human	Male	72	mL	333	279	53.8	16	306	247	59	19
*****	Human	Male	70	mL	339	276	62.6	18	345	244	101	29
*****	Human	Male	59	mL	237	181	55.8	24	241	176	65	27
Human Average	Human	N/A	66.25	mL	225	181	44	21	226	177	49	24

By definition, the closer the r^2 correlation value of the compared data and its equation's slope is to 1, as well as the Y Intercept and Mean difference in the results is to zero, the better match the results are, thus the more efficient the FlowQuant calculation algorithm is in comparison to 4DM. A closer look at the tables and graphs shows that the relationship between the 2 programs is exceptionally strong, showing high hopes for FlowQuant's validity versus 4DM which is currently considered as the current program of choice.

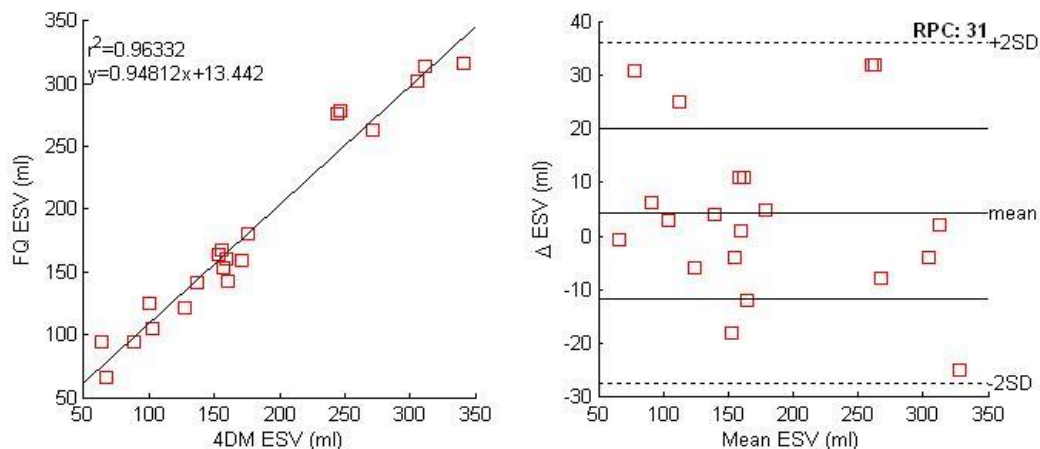
Each of the EDV, EDV and EF columns in FlowQuant are matched and compared with their corresponding column in 4DM using the Bland-Altman analysis method.

EDV Correlation (24 Rings)



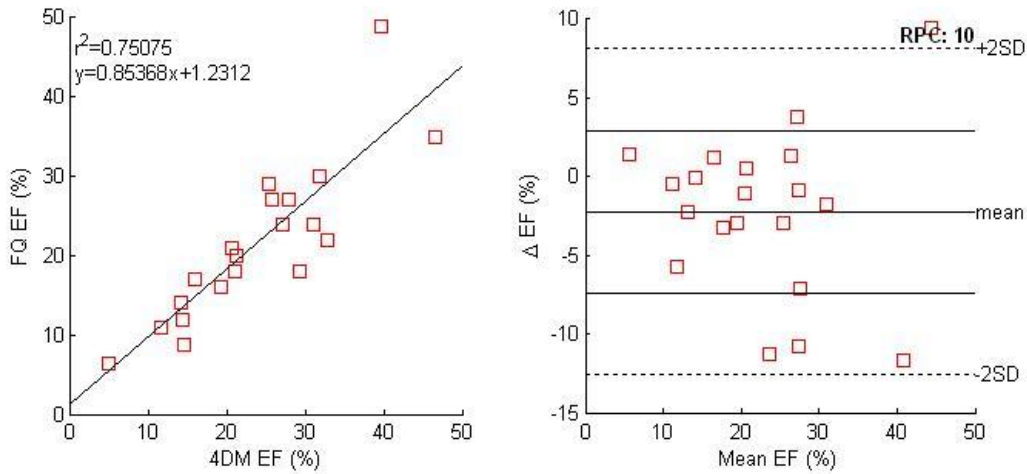
The previous figure show an EDV r^2 value near 0.97 which is remarkably fine (best r^2 value is 1), the line's slope similarly good (best slope value must be equal to 1), the y-intercept is relatively close to zero (18.3 is relatively a small amount in comparison to the y-values of the other points) and finally the mean difference in results estimated by both programs (in short the Mean Difference) is near -0.7 (see table below for values). That mean value shows a very negligible underestimation of the FlowQuant calculated EDV using these settings.

ESV Correlation (24 Rings)



The ESV comparison shows similarly good results, yet the slightly positive mean difference (4.265) implies a small overestimation of the ESV using these settings, most likely due to ignoring valve plane movement.

EF Correlation (24 Rings)



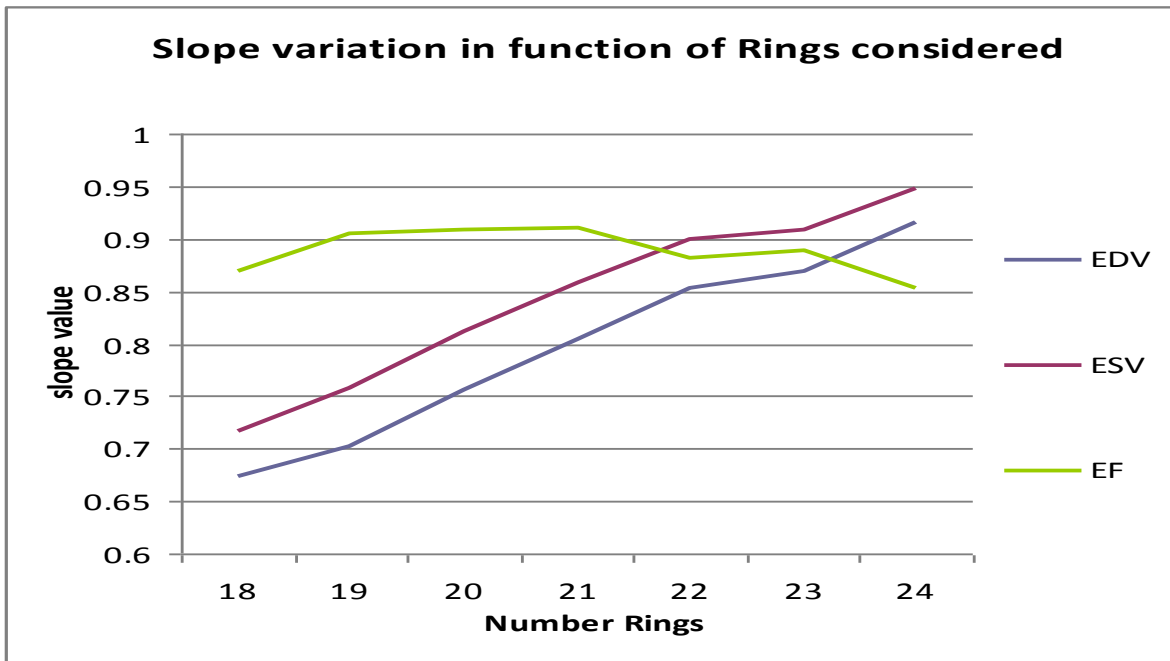
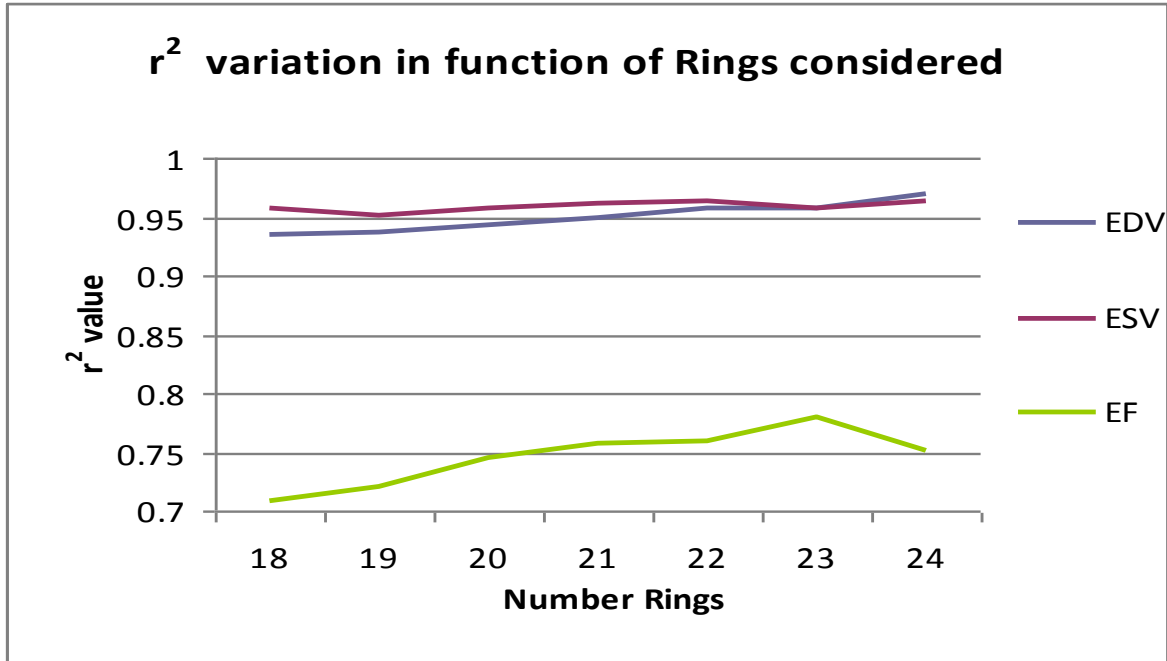
The EF correlation is strong as well, with a slight under estimation (slope =0.85 and mean difference near -2.235).

Due to lack of space, the table and graphs above show only the results computed when considering all 24 slices along the SA as stated previously. The same comparison test is simulated for different amount of rings taken into calculations, and the results are stored in the following table. The previous graphs illustrate the contents of the final row.

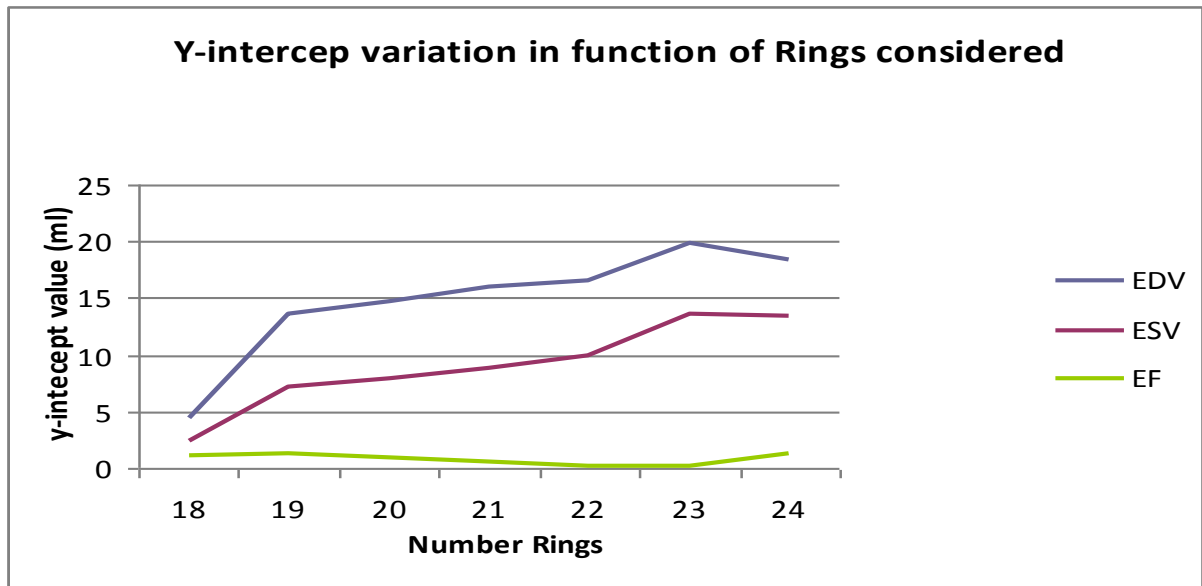
<u>Rings considered</u>	<u>EDV</u>			<u>ESV</u>			<u>EF (%)</u>		
	<u>r² value</u>	<u>Equation y=</u>	<u>Mean</u>	<u>r² value</u>	<u>Equation y=</u>	<u>Mean</u>	<u>r² value</u>	<u>Equation y=</u>	<u>Mean</u>
18	0.93569	0.67295x + 4.3938	-69.455	0.95617	0.71666x + 2.3687	-47.755	0.70895	Equation y=	-4.273393107
19	0.93691	0.70287x + 13.5318	-53.56	0.95094	0.75831x + 7.1752	-35.58	0.7207	Equation y=	-3.625170966
20	0.94277	0.75683x + 14.7071	-40.2	0.95672	0.81128x + 7.8691	-25.515	0.74389	Equation y=	-3.095170966
21	0.9496	0.80531x + 16.0605	-27.9	0.96079	0.85863x + 8.8683	-16.14	0.75659	Equation y=	-2.705170966
22	0.95701	0.85234x + 16.491	-16.85	0.96263	0.89964x + 9.9283	-7.825	0.75825	Equation y=	-2.520170966
23	0.95762	0.86956x + 19.9041	-9.55	0.95807	0.90876x + 13.6596	-2.48	0.78049	Equation y=	-2.415170966
24	0.96984	0.91579x + 18.3151	-0.7	0.96332	0.94812x + 13.442	4.265	0.75075	Equation y=	-2.235170966

The table shows the effect of the number of rings used in FQ calculations on the results computed. The best values are highlighted in yellow, and clearly it is seen for now that adopting all 24 rings of the LV in FlowQuant's calculations gives more similar results to 4DM's. This makes sense since the user who manually processes the scan in 4DM subconsciously sets the study range to include the entire LV from its apex to the edge of the lateral wall (the longest edge of the inclined plane which can be seen in the HLA and VLA slices). This provides a starting point for the algorithm to detect the valve plane location in 4DM, yet not its incline angle, whereas FlowQuant is still under development to acquire this property. Meanwhile, the valve plane is assumed to be at the 24th slice. On the other hand, the detection of the myocardium wall is done automatically in FlowQuant with the least user intervention, whereas in 4DM the detection relies greatly on user observation and expertise because of its manual aspect.

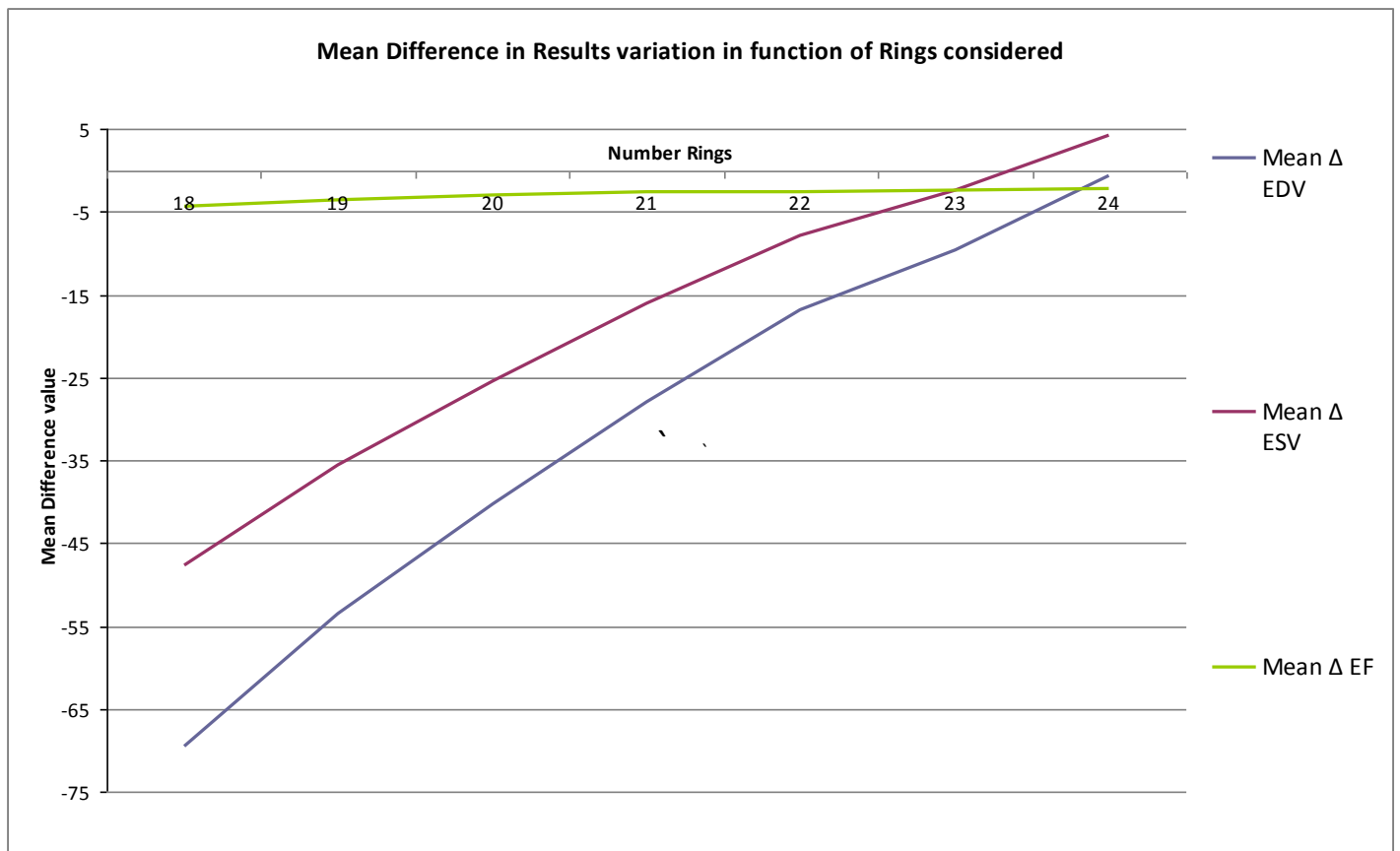
The following graphs show the variation of the correlation factors in respect to the number of rings considered during the volume computations. The r^2 values for the EDV and ESV don't vary greatly with different number of rings, whereas the EF r^2 value can vary with up to 0.08 units reaching its maximum at 23 slices.



A similar comparison for the equation's slope can be seen, for the EDV and ESV, the more rings considered, the nearest the slope it is to 1, yet the EF slope is the highest at 21 rings.



The EDV and ESV y-intercept comparison for different number of rings considered show values closest to zero with 18 rings and goes higher with the number of rings. However the values are still considered relatively minor in comparison to the high volume values.



Additional comment on Results and Comparison:

Another attempt at gathering random human scans must be made, yet cover a larger age range and include both healthy and defected heart scans. The program's validity must be verified in all possible cases. Having such spread out data should, theoretically, give a better insight on the correlation between both programs, whereas data of close range increase the error margin in the calculations. In addition, thorough Inner and Inter user variability tests must be made, to insure quality insurance as well as results' consistency when the program is used by different users or the same user multiple times. It has not been established yet, however the speculations are that FlowQuant's automation over 4DM's manual handling offers more consistency in its results, and less user intervention.

IV. FlowQuant advantage over 4DM:

FlowQuant is as automated as possible allowing the least user intervention, yet still holds extremely good agreement with 4DM results regardless of intervention. The results are not sensitive to the user in FlowQuant.

The automation is beneficial to routine clinic work allowing reduced workload, least or no inner-variability or inter-variability in FlowQuant whereas 4DM's manual dependence allows great variability each time the scan is processed. The experience using the program is not as essential in FlowQuant as it is to 4DM due its automation, whereas familiarity with manually defining the wall contours is indispensable to process the scan and obtaining acceptable results in 4DM.

It is safe to say that the updated version of FlowQuant, if continuously improved over time, can eventually even challenge 4DM to its title of "The Program of Choice".

C. UNIX Support Feature

I. Introduction

As for the second part of the workload done this summer, it is safe to acknowledge that UNIX platforms are currently considered the most reliable systems, since they provide very powerful servers that can run basically at non-stop rate, while handling a lot of studies at the same time. Therefore, UOHI sought to replace the current PC platforms with UNIX platforms for their reliability, an important factor to be considered at a vital location like a hospital, where any system failure can result in catastrophic consequences. To accommodate the hospital's needs of the new operating systems, FlowQuant was revised and modified to achieve the ability to work flawlessly on PC and on UNIX simultaneously.

II. Methodology

The UNIX operating system (Unix OS) holds certain characteristics that are not similar to PC OS. Among those characteristics are: The Case Sensitivity in UNIX, UNIX's forward slash versus PC's backward slash in directories names, UNIX specific paths and locations of particular files or tools.

1) Case Sensitivity Mismatch:

Since UNIX emphasizes on case sensitivity, running the FlowQuant program before on UNIX OS resulted in crashes, and logical errors, mainly due to the program's inability to locate certain files on the computer because of a case sensitivity mismatch in the file's name and the name used to in the code. PC operating systems do not take into account case sensitivity, therefore these error do not show on those platforms. In order to create a single version supporting both platforms, some hardcoded file names were modified to match the case sensitivity of the file name, whereas some other files were changed on the drive itself to overwrite their non-case-sensitive aliases, for faster editing of the program.

One point to consider from now on: during the implementation of later versions of FlowQuant, the programmers need to verify case sensitivity matching to avoid future errors.

2) Backward/Forward slash dilemma:

UNIX based operating systems use forward slashes to define a directory or file path location. Having hardcoded backward slashes results in similar errors to the ones created by case sensitivity mismatches. PC OS does not take into account the difference between two the slashes, therefore this error never popped up before. FlowQuant now adopts a function entitled "filesep" that can detect the type of the operating system currently available and return a forward or backward slash to serve requirements. A MANUAL search/modification of the hardcoded backward slashes had to be conducted word for word by me, changing all slashes into "filesep" calls.

3) UNIX paths and tools:

Unlike the PC operating system, the UNIX operating systems rely heavily on the Terminal console from which everything needed on the drive can be accessed and modified. To accommodate this characteristic, I modified the program in order to access certain paths, locations and files that either are located elsewhere, are named differently or do not exist on PC platforms. For instance, in order to issue a specific license approval for each computer that runs FlowQuant, the internet computer address is extracted to verify validity and issue the approval, however, the command used in the PC command window is “ipconfig” from which the desired internet address is read, whereas on UNIX/Linux computers it is called by the terminal using the “ifconfig-all” and then the desired internet address is found under another identification name that is different than PC’s.

To fix these sorts of problems, each case was studied separately, and Unix System knowledge was of large importance.

III. Limitations:

The Fedora 5 operating system that was already installed on the Unix platform computer created graphical errors on the figures employed by FlowQuant, since not the same graphical simulators are used on the different platforms.

Luckily, the newly released Fedora 9 accommodates these issues, and hasn’t shown any computer crashes so far, once it was updated.

The program is limited to the latest versions of UNIX operating systems, and user knowledge and expertise on working in a UNIX platforms environment is needed to set up the computer to its full potential and acceptance of FlowQuant.

D. Conclusion

The newly updated version of FlowQuant with its new features has proven itself user-friendly while defending its validity against 4DM. The Ejection Fraction and Wall Thickening calculating algorithm can be clinically approved for regular daily use, providing a very accurate insight on the patient’s heart condition and functionality and therefore determining proper treatment as soon as possible.

In addition, its UNIX compatibility can satisfy highly involved researchers’ need of dependable operating systems to run exhausting procedures without facing server meltdown, due to the highly recommended durably and reliance characteristics that Unix is famous for. Now, the thought of replacing the currently used PC platforms and installing FlowQuant on the Unix platform is thought. Now FlowQuant can run virtually on any operating system flawlessly, increasing the range of use of the program for commercial ease.

E. Copyrights and Acknowledgements:

During the COOP summer work term from May to August 2009, and the continuous development and update of FlowQuant, I was assisted by Mr. Ran Klein and supervised by Mr. Robert deKemp, to insure proper programming as well as time and quality efficiency. I do not in any way take credit for any features available in FlowQuant prior to the Gated Report I helped build: FlowQuant has been developed for years by fellow colleagues and I do not take credit for bringing the program to its current popularity. I acknowledge accessing their work to satisfy the main objectives sought, and any changes were confirmed by Mr. Ran Klein before merging my small modifications with their work.

The implementation of the Gated Report was solely my work alone, assisted by Mr. Ran Klein on technical emergencies however I do not deny any advices given to me by my superiors for quality insurance or unwanted deadlines. The notions available in this report should not be copied in any way or imitated without my consent.

*“I acknowledge that this report as well as its contents is purely my own work, with assistance and revision done by my supervisors stated above, any modification or editing to this report must be approved by myself and myself only. Also this report meets full confidentiality set by my supervisors and the University of Ottawa Heart Institute, and should not be made public in total or in part of any form, shape or content without consent from my behalf.
Any breach of the requests above will be considered as a violation to this copyright.”*

Stated by Charles Malo, August 2009

F. References

(1): Lars Stegger, Edwin Heijman, Klqus P.Schäfers, Klaas Nicolay, Michael A. Schäfers, and Gustav J.Strijkers, “Quantification of Left Ventricular Volumes and Ejection Fraction in Mice Using PET, compared with MRI”, The Journal of Nuclear Medicine, Vol.50, No.1, January 2009.

(2): Positron emission tomography. In Wikipedia: The Free Encyclopedia. Wikimedia Foundation Inc. Encyclopedia on-line. Available from http://en.wikipedia.org/wiki/Positron_emission_tomography, Internet. Retrieved September 2nd 2004.

(3): Matlab help section on the “poly2mask” function, © 1984-2007 The MathWorks, Inc .

G. Confidentiality Release